



Research Article

Agricultural Land Use Classification Using Vegetation Indices, PCA, and Google Earth Engine: Case Study of Söke/Aydın

Melis İnalpulat^{1,2*}  Neslişah Civelek^{2,3}  Metin Uşaklı^{2,4}  Levent Genç^{2,5} 

¹Agricultural Remote Sensing Laboratory (AGRESEL), Department of Agricultural Structures and Irrigation, Faculty of Agriculture, Çanakkale Onsekiz Mart University,

²Computer-Agriculture-Environment-Planning (ComAgEnPlan) Study Group, Çanakkale Onsekiz Mart University,

³Department of Geographical Information Technologies, School of Graduate Studies, Çanakkale Onsekiz Mart University,

⁴Department of Real Estate Development, School of Graduate Studies, Çanakkale Onsekiz Mart University,

⁵Land Use and Climate Change Laboratory (LULC-Lab), Department of Urban and Regional Planning, Faculty of Architecture and Design, Çanakkale Onsekiz Mart University.

*Corresponding author: melissacan@comu.edu.tr

Received Date: 10.05.2023

Accepted Date: 07.06.2023

Abstract

Land use and land cover (LULC) classification is known to be one of the most widely used indicators of environmental change and environmental degradation all over the world. There are various algorithms and methods for LULC classification, whereby reliability of the classification maps presents the principal concern. The study focused on evaluation of accuracies of LULC maps produced from original bands of Sentinel-2 imageries together with Normalized Difference Vegetation Index (NDVI), Green Normalized Difference Vegetation Index (GNDVI), and Principal Component Analysis (PCA) using Google Earth Engine (GEE) platform to identify best enhancing method for agricultural land use classification. Moreover, short-term LULC changes aimed to be identified in the specified area. To achieve the aims, all available imageries acquired in the same month of different years with less than 10% cloud contamination were used to compose averaged images for May 2018 and May 2022 for generating LULC₂₀₁₈ and LULC₂₀₂₂ maps. The area has separated into seven main classes, namely, olive (O), perennial cultivation (P), non-perennial cultivation (NP), forest (F), natural vegetation (N), settled area-bare land (SB), and water surface (W) via random forest algorithm. Reliabilities of LULC maps were evaluated through accuracy assessment procedures considering stratified randomized control points. Transitions between each LULC classes were identified.

Keywords: Agricultural land use, classification accuracy, Google Earth Engine, PCA, Sentinel-2, vegetation indices

Vejetasyon İndeksleri, Ana Bileşenler Analizi ve Google Earth Engine Kullanılarak Tarımsal Alan Kullanım Sınıflandırması: Söke/Aydın Örneği

Öz

Arazi kullanım ve arazi örtüsü (AKAÖ) sınıflaması çevresel değişim ve bozulmanın dünya genelinde en çok kullanılan göstergelerinden biri olarak bilinmektedir. AKAÖ sınıflaması için çeşitli algoritmalar ve metotlar var olup, en önemli hususların başında sınıflama haritalarının güvenliği gelmektedir. Çalışma, Google Earth Engine (GEE) platformu kullanılarak tarımsal sınıflama için en geliştirici metodu belirlemek için Sentinel-2 görüntülerinin original bantlarının yanında Normalize Edilmiş Farklılık Vejetasyon İndeksi (NDVI), Yeşil NDVI (GNDVI) ve Ana Bileşenler Analizi (ABA) ile üretilmiş AKAÖ haritalarının doğruluğunun değerlendirilmesi üzerine odaklanmıştır. Bunun yanında, seçilen alan içerisindeki kısa dönem AKAÖ değişimlerinin belirlenmesi amaçlanmıştır. Amaçlara ulaşabilmek için, farklı yılların aynı ayında alınmış olan bulutluluk oranı %10' dan az olan görüntüler kullanılarak AKAÖ₂₀₁₈ ve AKAÖ₂₀₂₂ haritaları elde edilmesi için Mayıs 2018 ve Mayıs 2022 için ortalama görüntüler oluşturulmuştur. Alan rassal orman (RO) algoritması ile zeytin (Z), ekili tarım (E), Dikili tarım (D), orman (O) doğal vejetasyon (DV), yerleşim alanı-çıplak alan (YÇ) ve su yüzeyi (S) olmak üzere yedi ana sınıfa ayrılmıştır. AKAÖ haritalarının güvenilirlikleri sınıf alanı büyüklüğüne göre rastgele dağıtılmış

kontrol noktaları göz önünde bulundurularak değerlendirilmiştir. Sınıfların birbirlerine dönüşümleri belirlenmiştir.

Anahtar Kelimeler: Ana Bileşenler Analizi, Google Earth Engine, Sentinel-2, sınıflama doğruluğu, tarımsal alan, vejetasyon indeksleri.

Introduction

Land use and land cover (LULC) change is a continuous phenomenon against natural events and anthropogenic activities, and has an essential role in monitoring of the alternations on the Earth surface. Human population declared to have exponential effects on land properties (Vivekananda et al., 2021). Starting from the industrial revaluation, population growth and urbanization trends have accelerated socioeconomic development in many areas. The situation also led to various environmental issues (Derdouri et al., 2021), such as ecosystem services, biodiversity, hydrological processes, and climate (Ahmet et al., 2009; Forkel et al., 2013; Usman et al., 2015; Hussain et al., 2022). The major part of LULC changes occur against urbanization, and usually led to loss of agricultural and natural vegetative covers (Dutta et al., 2020). Researchers from various disciplines have paid attention on human-environment interactions and LULC dynamics for better understanding of environmental processes and health (Kesgin-Atak and Ersoy-Tonyaloğlu, 2020). Monitoring of historical changes has great importance for a sustainable development, considering ecosystems and food security to maintain scarce resources.

Remote sensing technologies have long been used for LULC change detection by providing the data required for short-term and long term change analysis (El-kawy et al., 2019), with different spectral, spatial, radiometric, and temporal resolutions. On the other hand, the acceptability of LULC maps depends on their reliability (Rwanga and Ndambuki, 2017). Therefore, assessment of classification accuracy has become a primary step for remote sensing studies. Using appropriate techniques increase classification accuracy. However, selection of appropriate method, algorithm or bands for change detection presents a great challenge (Lu et al., 2004; Chughtai et al., 2021). As it is cited by Mallick and Rudra (2021), different algorithms including maximum likelihood (MLA), support vector machine (SVM) or random forest (RF), and indices like Normalized Difference Vegetation Index (NDVI), Normalized Difference Water Index (NDWI) have recently used for enhancing classification (Rawat et al., 2013; Maity et al., 2020). On the other hand, original bands generally correlate with one to other, thus, use of less number of non-correlated variables reduces the biases in classification stage, whereas principal component analysis (PCA) is widely preferred for this purpose (Balazs et al., 2018).

Expansion of available remote sensing data and developments in satellite sensor systems have increased access and study with time series datasets, at higher costs of time and labor, and thus, remote sensing studies have shifted from traditional software to cloud-based platforms (Vizzari, 2022). Among these geospatial analytic platforms, Google Earth Engine (GEE) presents a user-friendly interface and contains various data and algorithm library (Schmitt et al., 2019; Belcore et al., 2020; Lodato et al., 2023). Moreover, using GEE provides the advantage of making instant changes at any stage without repetition of whole process (Parente et al., 2019), and enables users to overcome the difficulties in management, storage, processing and analysis of data in a time, cost and labor effective way (Gorelick et al., 2017; Vizzari, 2022). Therefore, GEE became one of the most widely used platforms for image processing.

In present study, it was aimed to compose LULC maps from the original band images, NDVI and Green Normalized Difference Vegetation Index (GNDVI) added images, and PCA images for identification of more appropriate technique for agricultural land use classification, and to determine short-term (five-year) changes in agriculture-related LULC classes using the most reliable LULC map in Söke district of Aydın Province. Sentinel-2 imageries of May 2018 and May 2022 were used as the main data source. The RF algorithm was adopted for LULC classification, and accuracies of maps were determined considering the same reference points for a systematic assessment using GEE.

Materials and Methods

Study Area

The study was conducted in Söke district of Aydın province, Turkey. The center coordinates of the area is 37°45'7" N and 27°24'20" E. The area presents typical characteristics of Mediterranean

climate. The area was selected due to its importance in agricultural sector whereas many agricultural products can be grown due to suitable climate and soil conditions. Particularly, cotton, field crops, olive, citrus, and fig are known to be the main agricultural products in the area.

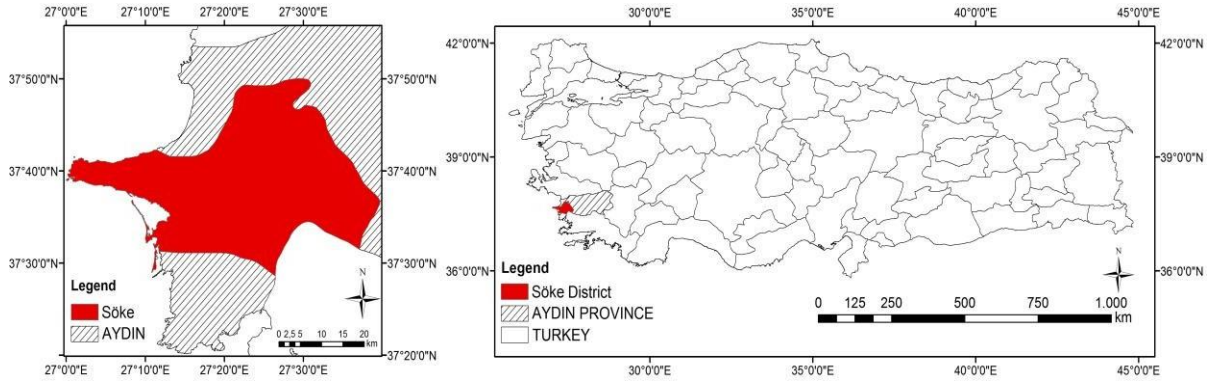


Figure 1. Location of Söke district within Aydın province and Turkey

Data Collection and Processing

Short-term LULC changes occurred in five-year period between 2018 and 2020 were identified through Sentinel-2 imageries. The years were selected depending on the alternations in areas and production amounts of perennial plants in the area (TÜİK, 2023). Sentinel-2 imageries acquired in May of 2018 and 2022 with cloud cover under 10% were used to obtain averaged images for the specified months. Bands of (2,3,4,5,6,7,8,8A,11, and 12) of each date were used to create original ten (10B) images. In present study, NDVI (Rouse et al., 1973) and GNDVI (Gitelson et al., 1996) images were generated (Eq. 1 and Eq. 2). In addition to original bands, NDVI and GNDVI were added prior to the classification whereas NIR, green and red bands were excluded, and new images were obtained including nine bands (9B) (Eq. 3). Moreover, 10B imagery was reduced into fewer bands using PCA (Eq. 4-9) (Estornell et al. (2013).

$$NDVI = \frac{B_{NIR} - B_{RED}}{B_{NIR} + B_{RED}} \quad (1)$$

$$GNDVI = \frac{B_{NIR} - B_{GREEN}}{B_{NIR} + B_{GREEN}} \quad (2)$$

$$9B = (10B - (B_{NIR}, B_{GREEN}, B_{RED}) + NDVI + GNDVI) \quad (3)$$

where, B_{NIR} , B_{RED} and B_{GREEN} represents NIR, red and green bands of Sentinel-2 imageries.

$$X_b = \begin{pmatrix} x_1 \\ x_2 \\ \vdots \\ x_{10} \end{pmatrix} \quad (4)$$

$$C_{b,b} = \begin{pmatrix} \sigma_{1,1} & \dots & \sigma_{1,10} \\ \vdots & \ddots & \vdots \\ \sigma_{10,1} & \dots & \sigma_{10,10} \end{pmatrix} \quad (5)$$

$$\sigma_{i,j} = \frac{1}{N-1} \sum_{p=1}^N (DN_{p,i} - \mu_i)(DN_{p,j} - \mu_j) \quad (6)$$

$$\det(C - \lambda I) = 0 \quad (7)$$

$$Y_{10} \begin{pmatrix} y_1 \\ y_2 \\ \vdots \\ y_{10} \end{pmatrix} = \begin{pmatrix} w_{1,1} & \dots & w_{1,10} \\ \vdots & \ddots & \vdots \\ w_{10,1} & \dots & w_{10,10} \end{pmatrix} = \begin{pmatrix} x_1 \\ x_2 \\ \vdots \\ x_{10} \end{pmatrix} \quad (8)$$

$$(C - \lambda_{10}I)w_{10} = 0 \quad (9)$$

Where X is vector of original data, X_b is simplified Sentinel-2 matrix, b is number of bands, C is covariance matrix, σ_{ij} is covariance of each bands' pair, $DN_{p,i}$ digital number of specified pixel (p) of a band (i), μ_i and μ_j are means DN's of B_i and B_j , λ is Eigenvalues, I is diagonal identity matrix, Y is PC vector, W is transformation matrix.

Image Classification, Accuracy Assessment, and Change Analysis

Original 10b, NDVI and PCA imageries were classified using RF algorithm via GEE platform to obtain LULC_{2018-10B}, LULC_{2018-9B}, LULC_{2022-9B}, LULC_{2018-PCA}, and LULC_{2022-PCA} maps. Main LULC classes were determined as, olive cultivation (O), perennial cultivation (P), non-perennial cultivation (NP), forest (F), natural vegetation (N), settled-bare area (SB), and water surface (W). Training samples are randomly collected and number of samples for each LULC class was altered depending on the magnitudes and complexity of classes (Table 1).

Table 1. Number of training samples for each year

Year/Class	W	NP	SB	P	O	N	F	Total
2018	209	632	1047	112	134	330	503	2967
2022	221	659	1054	112	164	432	518	3160

Subsequently, accuracies of LULC maps were determined according to Congalton and Green (2009). The assessment procedure refers to comparison of classified image and reference or ground-truth data for determination of LULC map pixels are well-classified or misclassified. Overall accuracy (OA) (%), overall kappa values (K), and user's accuracies (UA) (%) were calculated and compared to identify best performing imagery for agricultural land use classification.

Subsequent to the accuracy assessment procedures a post-classification change detection method is applied to most accurate LULC maps of 2018 and 2022. A post-classification change detection technique was used to evaluate 'from-to' changes occurred in short-term between 2018 and 2022 for calculation of gains and losses from different types of agricultural land uses.

Results and Discussion

Prior to the classifications, components from PCA were selected to the retain majority of the total variance depending on band weighting values for each component (%). The first three components of PCA₂₀₁₈ have represented 74.90 %, 19.44 %, 4.38 %, while the first three components of PCA₂₀₂₂ represent 64.18 %, 29.52, and 4.88 % of total variance with the same order. This situation has demonstrated that 98.77 % and 98.58 % of total variances for 2018 and 2022 can be presented using these components. Accordingly, three components were used in the PCA imagery of each year. Composed LULC maps are given in Figure 2a, b, Figure 3a, b, and Figure 4a, b.

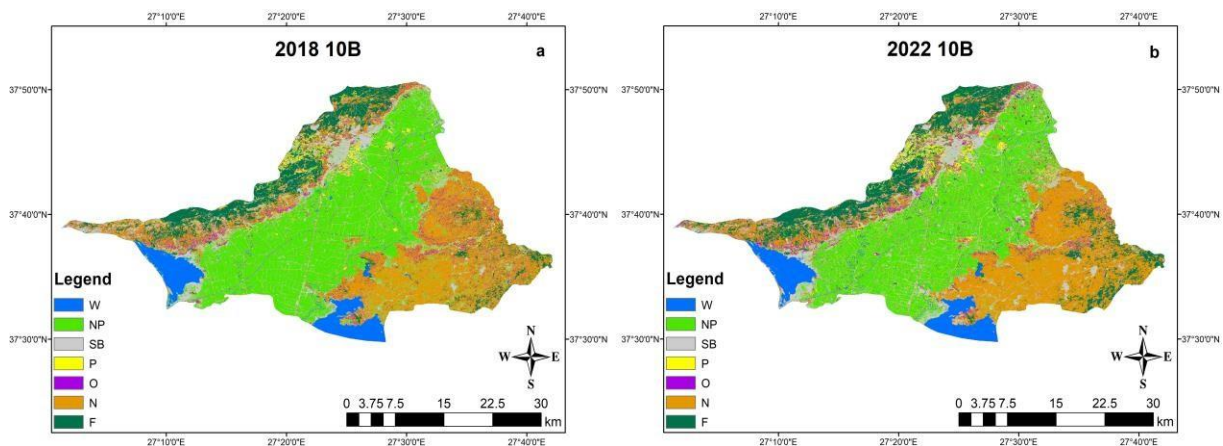


Figure 2. LULC maps derived from original 10B images a. LULC_{2018-10B}, b. LULC_{2022-10B}

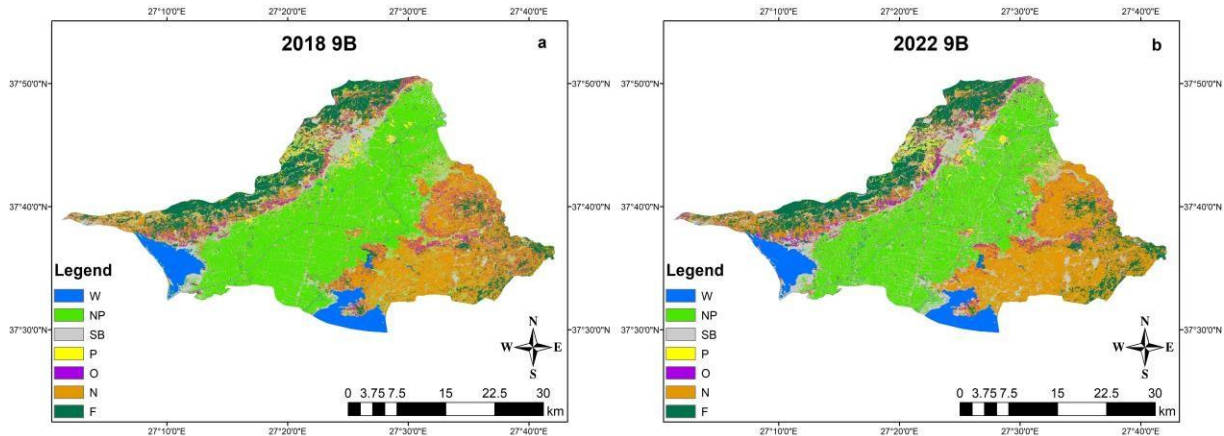


Figure 3. LULC maps derived from 9B images a. LULC_{2018-9B}, b. LULC_{2022-9B}

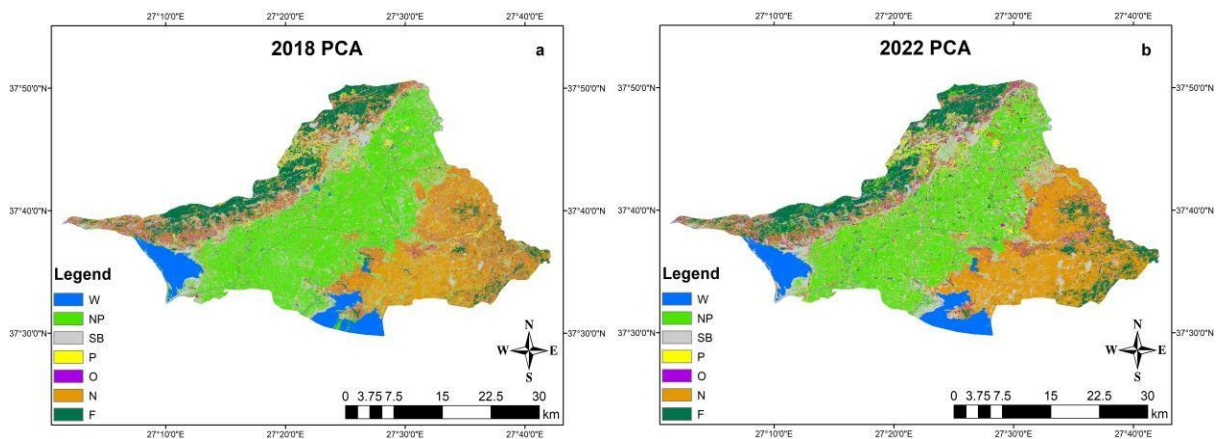


Figure 4. LULC maps derived from PCA images a. LULC_{2018-9B}, b. LULC_{2022-9B}

Areas of LULC classes were calculated depending on the LULC maps (Table 2). It was seen that there are noticeable differences in both magnitudes and directions of temporal changes between 10B, 9B and PCA-based classifications. Particularly, there are observable differences in agriculture-related classes, namely, NP, O and P, as well as SB class. The trends on change directions (-/+ and severities of LULC_{10B}, LULC_{9B} and LULC_{PCA} maps were considerably different. On this account, identification of most accurate LULC map has great importance for more reliable evaluation of the historical changes, and presents one of the most significant operations for determination of the quality of product (Rwanga and Ndambuki, 2017).

Table 2. 2018 and 2022 LULC class areas obtained from different band combinations (ha)

Class	LULC _{2018-10B}	LULC _{2022-10B}	LULC _{2018-9B}	LULC _{2022-9B}	LULC _{2018-PCA}	LULC _{2022-PCA}
W	6277	6363	6341	6350	6421	6654
NP	38877	33421	37672	33338	33316	29534
F	11358	13148	15280	12556	11297	13289
SB	14835	16150	12589	17853	21527	21247
O	4489	4137	5153	5308	5114	5329
P	3925	3770	3925	3039	3982	4362
N	26608	29380	25409	27925	24712	25954
Total	106369	106369	106369	106369	106369	106369

Table 3 shows the accuracies of derived LULC maps terms of OA, K, and UA. The OA and K values have shown that addition of NDVI and GNDVI bands instead of green, red and NIR bands have increased the classification accuracy in both years. This finding has revealed that addition of NDVI

and GNDVI may slightly improve reliability of the overall classification. However, individual user's accuracies of each class provide better indication for understanding the effects of applied methods on reliability of the specific classes. Adding NDVI and GNVI instead of green, red, and NIR bands has significantly increased accuracies of O and P classes, while a slight decrease occurred in NP. The findings were coherent with other studies since consideration of indices, such as NDVI and GNDVI, instead of original bands in classification models have recommended to be useful in agricultural and environmental studies (Yassine et al., 2021). In comparison, using PCA resulted in decreased accuracy levels in all agriculture-related classes in 2018. However, there was an observable increase in accuracy of O class in LULC_{2022-PCA}, which was sourced from the misclassifications of complex spectral structure in the natural olives around forest areas in 2018, while the reduction in NP and N classes were more drastic. As the LULC_{9B} maps of each year gave the most satisfactory results, the changes are determined considering LULC_{2018-9B} and LULC_{2022-9B}. Accordingly, F, NP and P classes have decreased by 2724 ha, 4334 ha, and 886 ha, respectively. In addition to these alternations, visual interpretations has revealed that agricultural related class, particularly P and O, seemed more dispersed with smaller patches, whereby increase of smaller number patches in agricultural classes also triggers increase in fragmentation (Lasanta et al., 2015), as similar situations have reported for İzmir province (Kara et. al., 2019). On contrary, areas of W, SB, N, and O classes were increased by 9 ha, 5264 ha, 2516 ha, and 155 ha.

Table 3. Total and class accuracy indicators of 2018 LULC maps

Classes	LULC _{2018-10B}	LULC _{2018-9B}	LULC _{2018-PCA}	LULC _{2022-10B}	LULC _{2022-9B}	LULC _{2022-PCA}
	UA (%)	UA (%)	UA (%)	UA (%)	UA (%)	UA (%)
W	100.00	99.13	100.00	93.35	99.17	98.32
NP	98.49	99.24	92.06	96.11	96.88	87.64
F	96.64	96.64	94.17	97.98	98.39	93.23
SB	90.07	93.05	83.17	95.04	95.04	88.68
O	96.15	96.23	76.67	84.88	81.05	81.82
P	87.84	88.46	75.32	80.00	86.15	77.63
N	87.28	90.59	82.84	85.59	89.50	84.23
OA(%)	94.51	95.05	87.38	93.14	94.14	88.33
K	0.9323	0.9391	0.8541	0.9165	0.9287	0.8584

Finally, the transformations between LULC classes have gathered from transition matrix of LULC_{2018-9B} and LULC_{2022-9B} (Table 4). Consideration of agricultural land use classes of NP, and P have revealed that main part of losses from these classes were consisted of transitions to SB class, demonstrating that LULC₂₀₁₈ NP and P class served as spaces for new SB areas with a total of 5800 ha. Major part of transitions of LULC₂₀₁₈ O class was into N class in until 2022 (982 ha). This situation sourced from decrease in greenness of shrubs under natural olive trees and classified as N class whereby coverages of olive trees were difficult to differentiate and misclassified, thus, overestimated in LULC₂₀₁₈ which can also be seen from the UA of LULC₂₀₁₈ O class. The gains from SB areas from agricultural classes were followed by gains from N class with an area of 1537 ha. In addition to transitions of N class into SB, a part of the class has started to use for agricultural production purposes in different ways (NP, P, and O). Similar situations have occurred in SB class since there were transitions from bare lands into agriculture. On the other hand, the transitions in W class sourced from alternations in of water level. Moreover, changes in marshlands and mine pits seemed responsible for the changes from different LULC types, especially in F and N class, where the canopy cover gave identical spectral signatures with each other due to changes in wetness or dryness levels of the soils located at such exceptional sites. Thus, the water content of the plants dependently affected, and the situations have directly impacted the reflectance characteristics. The losses in vegetative covers from forests and other natural vegetation, as well as agricultural lands, have resulted in increased land surface temperatures in Aydın province (Kesgin-Atak and Ersoy-Tonyalıoğlu, 2020). The alternations in meteorological parameters believed to be responsible for such situations.

Table 4. Transitions matrix showing gains and losses from each LULC class between 2018 and 2022

Class ₂₀₁₈₋₂₀₂₂	W	NP	SB	P	O	N	F	Total
W	5735	93	108	13	32	174	186	6341
NP	44	29949	5124	547	587	1327	94	37672
SB	24	1148	8641	384	594	1622	176	12589
P	21	468	676	1227	328	657	548	3925
O	4	321	547	193	2942	982	164	5153
N	54	486	1537	478	1841	19126	1887	25409
F	221	274	476	568	196	1557	11978	15280
Total	6323	33078	17847	2963	5657	27842	12659	106369

Conclusions

The study aimed to evaluate the use of two vegetation indices of NDVI and GNDVI, and PCA for enhancing classification accuracies of specified agricultural land use classes of NP, P and O, and to determine the changes occurred between 2018 and 2022 years depending on the LULC maps with highest accuracy in Söke district of Aydın province, Turkey. Findings have revealed that adding NDVI and GNDVI images instead of green, red and NIR bands have increased both OA and UA with higher K value and concluded to have potential to be used for NP and P classifications in Aegean-Mediterranean coast of Turkey under similar climate, soil and vegetative cover conditions. The difficulty of discriminating natural olives from other natural vegetation cover presented the major handicap of the study especially in 2022 due to altered meteorological conditions. Accurate LULC maps enables reliable monitoring of past changes, not only for detecting and solving current problems, but also for enhancing ongoing management strategies, and forecasting future situations for agricultural lands. Depending on the most reliable maps of LULC_{2018-9B} and LULC_{2022-9B}, it was seen that there were considerable decreases in NP and P class with over 7000 ha, while O class increased (155 ha). The SB areas have expanded by 5264 ha during the considered years and agricultural related classes comprised place for majority of recent settlements with a total area of 6347 ha. Using GEE provided an efficient and rapid tool for mapping LULC changes, particularly for agricultural land use with high accuracies. Moreover, the codes can be used for future studies with different variables such as samples or datasets. In conclusion, adoption of more controlled development strategies concluded to have great importance for maintenance of vulnerable and environmentally valuable ecosystems in the future, whereas VIs have recommended to be important components of agricultural classification, particularly in the areas with complex production pattern as well as the study area.

Author Contributions

All authors have participated in the work and take responsibility for the manuscript content.

Conflicts of Interests Statement

The authors declare no conflicts of interests.

Kaynaklar

- Ahmed, J., Ahmed, M., Laghari, A., Lohana, W., Ali, S., Fatmi, Z., 2009. Public private mix model in enhancing tuberculosis case detection in District Thatta, Sindh, Pakistan. *J. Pak. Med. Assoc.* 59(2): 82.
- Balazs, B., Biro, T., Dyke, G., Singh, S.K., Szabo, S., 2018. Extracting water-related features using reflectance data and principal component analysis of Landsat images. *Hydrological Sciences Journal.* 63(2): 269-284.
- Belcore, E., Piras, M., Wozniak, E., 2020. Specific Alpine environment land cover classification methodology: Google Earth Engine processing for Sentinel-2 data. *Int. Arch. Photogramm. Remote Sens. Spat. Inf. Sci.* XLIII-B3-2: 663-670.
- Chughtai, A.H., Abbasi, H., Karas, I.R., 2021. A review on change detection method and accuracy assessment for land use land cover. *Remote Sensing Applications: Society and Environment.* 22: 100482.
- Congalton, R.G., Green, K., 2009. Assessing the accuracy of remotely sensed data: principles and practices. *Photogramm. Rec.* <https://doi.org/10.1111/j.1477-9730.2010.005742.x>.
- Derdouri, A., Wang, R., Murayama, Y., Osaragi, T., 2021. Understanding the links between lulc changes and SUHI in Cities: Insights from two-decadal studies (2001–2020). *Remote Sensing.* 13: 3654.

- Dutta, V., 2012. Land use dynamics and peri-urban growth characteristics: Reflections on master plan and urban suitability from a sprawling north Indian city. *Environment and Urbanization ASIA*. 3(2): 277-301.
- El-kawy, A.O.R., Ismail, H.A., Yehia, H.M., Allam, M.A., 2019. Temporal detection and prediction of agricultural land consumption by urbanization using remote sensing. *Egypt. J. Remote. Sens. Space Sci.* <https://doi.org/10.1016/j.ejrs.2019.05.001>.
- Estornell, J., Marti-Gavila, J.M., Sebastia, M.T., Mengual, J., 2013. Principal component analysis applied to remote sensing. *Modelling in Science Education and Learning*. 6(2/7): 83-89.
- Forkel, M., Carvalhais, N., Verbesselt, J., Mahecha, M., Neigh, C., Reichstein, M., 2013. Trend change detection in NDVI time series: effects of inter-annual variability and methodology. *Remote Sensing*. 5(5): 2113-2144.
- Gorelick, N., Hancher, M., Dixon, M., Ilyushchenko, S., Thau, D., Moore, R., 2017. Google Earth Engine: Planetary-scale geospatial analysis for everyone. *Remote Sens. Environ.* 202: 18-27.
- Gitelson, A.A., Kaufman, Y.J., Merzlyak, M.N., 1996. Use of a green channel in remote sensing of global vegetation from EOS-MODIS. *Remote Sens. Environ.* 58: 289-298.
- Hussain, S., Mubeen, M., Karuppanan, S., 2022. Land use and land cover (LULC) change analysis using TM, ETM+ and OLI Landsat images in district of Okara, Punjab, Pakistan. *Physics and Chemistry of the Earth*. 126: 103117.
- Kara, B., 2019. Agrarian and wetland areas under metropolitan threats: learning from the case of Inciralti, Izmir (Turkey). *Applied Ecology and Environmental Research*. 17(6): 15087-151102.
- Kesgin-Atak, B., Ersoy-Tonyaloğlu, E., 2020. Monitoring the spatiotemporal changes in regional ecosystem health: A case study in Izmir, Turkey. *Environ. Monit. Assess.* 192: 385.
- Kesgin-Atak, B., Ersoy-Tonyaloğlu, E., 2020. Evaluation of the effect of land use/land cover and vegetation cover change on land surface temperature: The case of Aydın province. *Turkish Journal of Forestry*. 21(4): 489-497
- Lasanta, T., Nadal-Romero, E., Arnáez, J., 2015. Managing abandoned farmland to control the impact of re-vegetation on the environment. The state of the art in Europe. *Environmental Science & Policy*. 52: 99-109.
- Liu, J., Pattey, E., and Jégo, G., 2012. Assessment of vegetation indices for regional crop green LAI estimation from Landsat images over multiple growing seasons. *Remote Sensing of Environment*. 123: 347–358.
- Lodato, F., Colonna, N., Pennazza, G., Praticò, S., Santonico, M., Vollero, L., Pollino, M., 2023. Analysis of the spatiotemporal urban expansion of the Rome Coastline through GEE and RF Algorithm, Using Landsat imagery. *ISPRS Int. J. Geo-Inf.* 12: 141.
- Lu, D., Mausel, P., Brondízio, E., Moran, E., 2004. Change detection techniques. *Int. J. Rem. Sens.* 25(12): 2365-2401.
- Maity, B., Mallick, S.K., Rudra, S., 2020. Spatiotemporal dynamics of urban landscape in Asansol municipal corporation, West Bengal, India: a geospatial analysis. *GeoJournal*. <https://doi.org/10.1007/s10708-020-10315-z>.
- Mallick, K.S., Rudra, S., 2021. Land use changes and its impact on biophysical environment: Study on a river bank. *The Egyptian Journal of Remote Sensing and Space Sciences*. 24: 1037-1049.
- Parente, L., Taquary, E., Silva, A.P., Souza, C., Ferreira, L., 2019. Next generation mapping: Combining deep learning, cloud computing, and big remote sensing data, *Remote Sens.* 11(23): 2881.
- Rawat, J.S., Biswas, V., Kumar, M., 2013. Changes in land use/cover using geospatial techniques: A case study of Ramnagar town area, district Nainital, Uttarakhand, India. *Egypt. J. Remote Sensing Space Sci.* 16(1): 111-117.
- Rouse, J.W., Haas, R.H., Schell, J.A., Deering, D.W., 1973. Monitoring vegetation systems in the great plains with ERTS (Earth Resources Technology Satellite). *Proceedings of 3rd Earth Resources Technology Satellite Symposium*.
- Rwanga, S.S., Ndambuki, J.M., 2017. Accuracy assessment of land use/land cover classification using remote sensing and GIS. *Int. J. Geosci.* 8: 611-622.
- Salem, M., Tsurusaki, N., Divigalpitiya, P., 2021. Remote sensing-based detection of agricultural land losses around Greater Cairo since the Egyptian revolution of 2011. *97(2020)*: 1-8.
- Schmitt, M., Hughes, L.H., Qiu, C., Zhu, X.X., 2019. Aggregating cloud-free Sentinel-2 Images with Google Earth Engine. *ISPRS Ann. Photogramm. Remote Sens. Spat. Inf. Sci.* IV-2/W7: 145–152.
- TÜİK, 2023. Türkiye İstatistik Kurumu, İlçe bazlı bitkisel üretim istatistikleri. <https://biruni.tuik.gov.tr/medas/?locale=tr>, (08.05.2023)
- Usman, M., Liedl, R., Shahid, M.A., Abbas, A., 2015. Land use/land cover classification and its change detection using multi-temporal MODIS NDVI data. *J. Geosci.* 25(12): 1479-1506.
- Vivekananda, G.M., Swathi, R., Sujith, A.V.L.N., 2021. Multi-temporal image analysis for LULC classification and change detection. *European Journal of Remote Sensing*. 54(Supp.2): 189-199.

Vizzari, M., 2022. PlanetScope, Sentinel-2, and Sentinel-1 data integration for object-based land cover classification in Google Earth Engine. *Remote Sens.* 14: 2628.

Yassine, H., Tout, K., Jaber, M., 2021. The International Archives of the Photogrammetry, Remote Sensing and Spatial Information Sciences, Volume XLIII-B3-2021, XXIV ISPRS Congress.